Real-time measurement of atmospheric parameters for the 127-element adaptive optics system of 1.8-m telescope

Jie Mu (母 杰)[1,2,3*], Wenjia Zheng (郑文佳)[1,2], Mei Li (李 梅)[1,2], and Changhui Rao (饶长辉)[1,2]

[1]*Laboratory on Adaptive Optics, Institute of Optics and Electronics, Chinese Academy of Sciences, Chengdu 610209, China*

[2]*Key Laboratory on Adaptive Optics, Chinese Academy of Sciences, Chengdu 610209, China*

[3]*Graduate University of Chinese Academy of Sciences, Beijing 100049, China*

[*]*Corresponding author: mujiebest@163.com*

Received May 3, 2012; accepted July 10, 2012; posted online September 14, 2012

A real-time method for measuring atmospheric parameters based on co-processor field-programmable gate array (FPGA) and main processor digital signal processing (DSP) is proposed for ground-based telescopes with adaptive optics (AO) systems. Coherence length, outer scale, average wind speed, and coherence time are estimated according to closed-loop data on the residual slopes and the corrected voltages of AO systems. This letter introduces the principle and architecture design of the proposed method, which is successfully applied in the 127-element AO system of the 1.8-m telescope of Yunnan Astronomical Observatory. The method enables real-time atmospheric observations with the same object and path of the AO system. This method is also applicable to extended objects.

OCIS codes: 010.1080, 010.1330, 110.1080, 200.4560.

doi: 10.3788/COL201210.120101.

Atmospheric turbulence parameters are primary factors in astronomical site surveys. For instance, the site survey project in western China[1,2], the telescope plans for Antarctic Dome A[3,4], and the new-generation solar telescope site survey[5] for astronomical observations are all based on the evaluation of atmospheric turbulence parameters. Given that atmospheric conditions rapidly change, atmospheric turbulence considerably fluctuates with time. Although adaptive optics (AO) systems can be used to correct the dynamic wave-front distortion caused by atmospheric turbulence, the resolution of a telescope continues to be affected by atmospheric turbulence[6]. Hence, the real-time monitoring and recording of atmosphere turbulence parameters can improve AO systems.

Outer scale L_0, average wind speed v, coherence length r_0, and coherence time t_0 are used to describe atmospheric turbulence. The traditional method of measuring atmospheric parameters is the differential image motion monitor (DIMM) method[7,8], but it is suitable only for fixed objects. Moreover, the r_0 and L_0 measured by DIMM do not correspond to the same type of atmospheric turbulence, which is corrected by AO systems. Nasmyth adptive optics system (NAOS) uses six digital signal processings (DSPs) to calculate the abovementioned parameters[9], but some frames are lost because NAOS is limited by the processing speed of DSP (TMS320C40). In standard platform for adptive optics real-time applications (SPARTA), the processor cluster is used to calculate the atmospheric parameters[10], but the sampling frequency of the AO system is limited by Ethernet speed. To address these problems, we propose a real-time measurement system based on field-programmable gate array (FPGA) and DSP. In the system, open-loop data can be reconstructed rapidly by FPGA with the pipelining and multi-channel technique, after which atmospheric parameters can be calculated by DSP. This measurement method is successfully applied in the 127-element AO system installed on a 1.8-m telescope that the Yunnan Astronomical Observatory uses for stellar observations.

Measuring the atmospheric parameters in a closed-looped AO system necessitates the recovery of information on atmospheric turbulence. According to the controlling relationship in an AO system, (k-2)th frame open-loop Zernike coefficients $\{a_{i,\,\mathrm{rec}}^{k-2}\}$ can be reconstructed from kth frame residual slopes $\{g_j^k\}$ and (k-2)th frame corrected voltages $\{u_j^{k-2}\}$[11]:

$$\{a_{i,\,\mathrm{rec}}^{k-2}\} = \mathrm{VZ}\{u_j^{k-2}\} + \mathrm{SZ}\{g_j^k\}, \tag{1}$$

where SZ is the projection matrix of residual slopes and VZ is the projection matrix of corrected voltages.

The continuous L frames of the reconstructed open-loop Zernike coefficients $\{a_{i,\,\mathrm{rec}}\}$ are regarded as a group for temporal autocorrelation $C_{i,\,\mathrm{rec}}(\tau)$. Because noise and atmospheric turbulence are temporally decorrelated, $C_{i,\,\mathrm{rec}}(\tau)$ can be written as[11]

$$\begin{cases} C_{i,\,\mathrm{rec}}(\tau) = \langle a_{i,\,\mathrm{rec}}(t) a_{i,\,\mathrm{rec}}(t+\tau)\rangle \\ C_{i,\,\mathrm{rec}}(\tau) = C_{i,\,\mathrm{turb}}(\tau) + \sigma^2_{a_{i,\,\mathrm{noise}}}\delta(\tau) \end{cases}, \tag{2}$$

where $\sigma^2_{a_{i,\,\mathrm{noise}}}$ is the noise variance and $\delta(t)$ is the Dirac function. A fit of $C_{i,\,\mathrm{rec}}(\tau)$ $(\tau) > 0$ enables the estimation of $C_{i,\,\mathrm{turb}}(0)$ by extrapolation. The difference between $C_{i,\,\mathrm{rec}}(0)$ and $C_{i,\,\mathrm{turb}}(0)$ yields $\sigma^2_{a_{i,\,\mathrm{noise}}}$. Hence, we can obtain the real-time open-loop Zernike coefficient variance $\sigma^2_{a_{i,\,\mathrm{rec}}}$, with the noise variance removed.

According to Noll[10], atmospheric turbulence variance $\sigma^2_{a_{i,\,\mathrm{turb},p}}$ only depends on radial order p (the parameter that reflects the radial spatial frequency of Zernike polynomials). Thus, it can be derived from the average of all $\sigma^2_{a_{i,\,\mathrm{rec}}}$ values across radial orders. The relationship

among $\sigma^2_{\mathrm{turb},p}$, r_0, and L_0 is given by[11,12,13]

$$\begin{cases} \sigma^2_{\mathrm{turb},p=2} = 2.34\times10^{-2}\left(\dfrac{D}{r_0}\right)^{5/3} \\ \quad \times\left[1-0.39\times\left(\dfrac{2\pi D}{L_0}\right)+0.27\left(\dfrac{2\pi D}{L_0}\right)^{7/3}\right] \\ \sigma^2_{\mathrm{turb},p\geqslant3} = 0.756(p+1)\dfrac{\Gamma[p-5/6]}{\Gamma[p+23/6]}\left(\dfrac{D}{r_0}\right)^{5/3} \\ \quad \times\left[1-\dfrac{0.38}{(p-\frac{11}{6})(p+\frac{23}{6})}\left(\dfrac{2\pi D}{L_0}\right)^{2}\right] \end{cases}, \quad (3)$$

where D is the diameter of the telescope. To obtain r_0 and L_0, Eq. (3) should be simplified thus

$$\begin{bmatrix} \left(\dfrac{D}{r_0}\right)^{5/3} \\ \left(\dfrac{D}{r_0}\right)^{5/3}\left(\dfrac{2\pi D}{L_0}\right)^{2} \end{bmatrix} = \begin{bmatrix} d_{1,1} & \cdots & d_{1,pp-2} \\ d_{2,1} & \cdots & d_{2,pp-2} \end{bmatrix} \times \begin{bmatrix} \sigma^2_{\mathrm{turb},p=3} \\ \sigma^2_{\mathrm{turb},p=pp} \end{bmatrix}, \quad (4)$$

where pp is the maximum radial order, and matrix $\begin{bmatrix} d_{1,1} & \cdots & d_{1,pp-2} \\ d_{2,1} & \cdots & d_{2,pp-2} \end{bmatrix}$ is fixed for a specific AO system; this matrix can be obtained from Eq. (3).

A cut-off period τ_i for each open-loop Zernike coefficient is derived from the $1/e$ width of its temporal autocorrelation. According to Taylor's hypothesis of a frozen turbulence, an average wind speed v can be computed from all cut-off periods τ_n; this value is the average of τ_i across radial orders[11]:

$$v = \frac{1.15\pi D\Sigma(p+1)\tau_n^{-1}}{0.3\Sigma(p+1)^2}. \quad (5)$$

Coherence time t_0 is calculated from r_0 and v[14]:

$$t_0 = 0.31 r_0/v. \quad (6)$$

Figure 1 shows the architecture of the AO system with the real-time measurement scheme. The wave-front distortion is detected by the wave-front sensor. Digital residual slopes and digital corrected voltages are obtained by the wave-front processor. These data are split into two channels.

In the first channel, the digital corrected voltages are passed into D/A for digital-analog conversion. The analog corrected voltages are amplified by a high-voltage amplifier. Then, a tip-tilt mirror (TM) and a deformable mirror (DM) are driven by the high corrected voltages to compensate for wave-front distortion.

In the second channel, the digital residual slopes and digital corrected voltages (residual slopes and corrected voltages hereafter for brevity) are transmitted into the real-time measurement system to calculate the atmospheric parameters in real time. These atmospheric parameters can then be transmitted to the host computer by compact peripheral component interconnect (CPCI) bus or Ethernet.

The real-time measurement system is composed of a co-processor FPGA, a main processor DSP, and memory. The types of memory available are static random access memory (SRAM), synchronous dynamic random access memory (SDRAM), and FLASH. In the proposed system, pipelining in the time dimension and multi-channel computing in the spatial dimension are applied. The open-loop Zernike coefficients are reconstructed by the FPGA on the basis of the closed-loop data on the residual slopes and corrected voltages. At the core of FPGA, the processing element consists of a multiplier and an accumulator (Fig. 2). The continuous multi-frame data on the open-loop Zernike coefficients are regarded as a group for statistical calculations, including temporal autocorrelation, noise removal, and variance. The atmospheric parameters are calculated by the DSP by using these continuous multi-frame data. Many optimization methods are used to improve the processing performance of DSP; such methods include the use of library functions, compilers, caches, enhanced direct memory access (EDMA3), and inline functions. For the seamless caching of the reconstructed open-loop Zernike coefficients, the SRAM used exhibits a ping-pong structure. SDRAM is used to store operation data on DSP. In addition, flash modules realize the booting of FPGA and DSP when power is on.

Given that FPGA and DSP are arranged in a pipeline and assuming that the continuous L frames of the open-loop Zernike coefficients are a group, (Q-1)th group data are used in statistical calculations for atmospheric

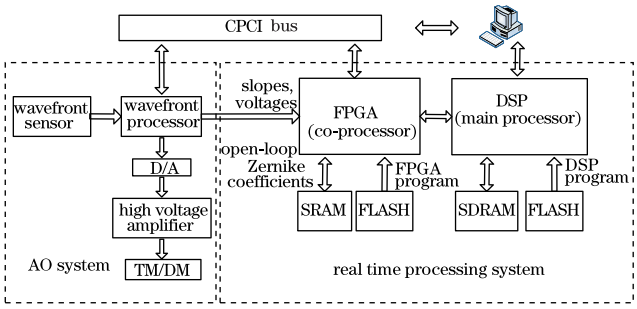

Fig. 1. Block diagram of the AO system with real-time measurement system.

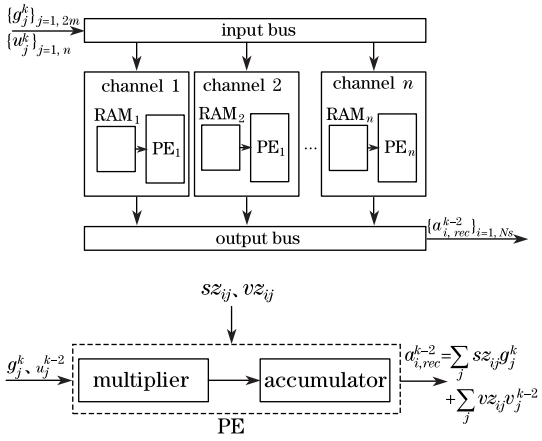

Fig. 2. Architecture design of FPGA; m is the number of valid sub-apertures; n is the number of actuators; N_s is the Zernike order.

parameters by DSP when Qth group data are reconstructed by FPGA. To ensure real-time computation, the processing latency of FPGA (Δt_1) should be less than 1/fs (fs is the sampling frequency of the AO system). In the meantime, the processing latency of DSP (Δt_2) should be less than L/fs. For the 127-element AO system, Δt_1 is 19.65 μs when 7 parallel channels are created with a 100-MHz processing clock, and Δt_2 is 553.8 ms when 3700 frames of the open-loop Zernike coefficients are used for statistical calculations. The sampling frequency of the AO system is no more than 2000 Hz, indicating that the real-time measurement system satisfies the requirements of real-time computing and possesses a considerable design margin. The atmospheric parameters are refreshed at least every 1.85 s. The timing sequence is shown in Fig. 3.

The real-time measurement system is applied in the 127-element AO system of the 1.8-m telescope of Yunnan Astronomical Observatory. In the AO system, a wave-front processor with a sampling frequency of 500 to 2000 Hz, a wave-front sensor with 128 valid sub-apertures, and a DM with 127 active actuators are used. The arrangement of the wave-front sensor sub-apertures and the DM actuators is shown in Fig. 4.

Figure 5 shows the atmospheric parameter observation on r_0 (Fig. 5(a)), L_0 (Fig. 5(b)), v (Fig. 5(c)), and t_0 (Fig. 5(d)) for a star, whose magnitude (Mv) is 2.56 when the AO system is in closed-loop mode. The values of r_0, L_0, v, and t_0 are between 5 and 10 cm (mean value, 7.9 cm), between 4 and 15 m (mean value, 6.4 m), between 2 and 10 m/s (mean value, 3.5 m/s), and between 2 and 13 ms (mean value, 8.8 ms), respectively. All these values are within the reasonable range of previous experimental observations. These results indicate that the system can be used for the real-time measurement of atmospheric parameters in a closed-loop AO system.

The correction effectiveness of the AO system for atmospheric turbulence is depicted in Fig. 6 at different seeing. For the first group of stars (Fig. 6(a)), the mean

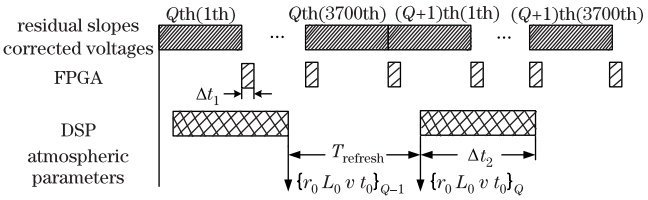

Fig. 3. Signal timing sequence.

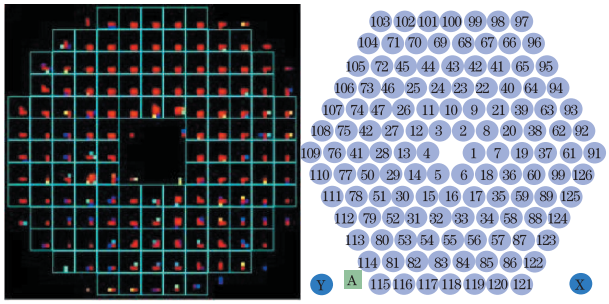

Fig. 4. Arrangement of sub-apertures and actuator layout of the 127-element AO system.

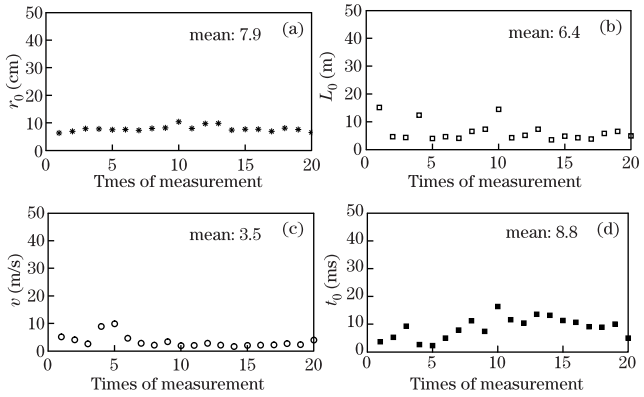

Fig. 5. Atmospheric parameters (a) r_0, (b) L_0, (c) v, and (d) t_0 for a star (Mv=2.56).

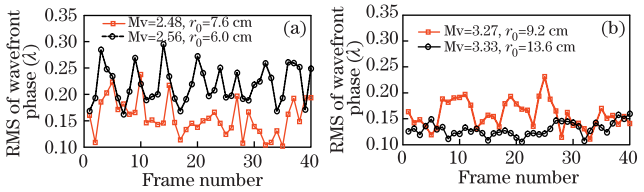

Fig. 6. RMS of the wave-front phase under different seeing conditions.

residual root square (RMS) of the wave-front phase is 0.22 λ at r_0 of 6.3 cm, and 0.16 λ at r_0 of 7.6 cm. For the second group of stars (Fig. 6(b)), the mean residual RMS of the wave-front phase is 0.16 λ when r_0 is 9.2 cm, and 0.13 λ when r_0 is 13.6 cm. λ denotes the wavelength. The results show that a better seeing (large r_0) results in a smaller residual RMS of the wave-front phase, indicating that the ability of the AO system to compensate for atmospheric turbulence is related to the seeing of the atmosphere; that is as seeing become better, compensation for atmospheric turbulence improves.

The above-mentioned results are obtained from point objects. The method is also applicable to extended objects.

In conclusion, a real-time method for measuring the atmospheric parameters of ground-based telescopes with AO systems is proposed. The proposed method is applied in the 127-element AO system of a 1.8-m telescope to calculate outer scale L_0, average wind speed v, coherence length r_0, and coherence time t_0. The results confirm that the method is suitable for the real-time measurement atmospheric parameters in a closed-loop AO system. In addition, the ability of the AO system to compensate for atmospheric turbulence is related to seeing conditions. The processing latencies of FPGA and DSP are 19.65 μs and 553.8 ms, respectively. The time spent refreshing the atmospheric parameters is no more than 1.85 s. The method is applicable to both point and extended objects.

This work was supported by the National Natural Science Foundation of China under Grant No. 11178004.

References

1. Y. Yao, The Astronomical Site Survey in West China, J. Korean A. S. 39 (2005).

2. T. Sasaki, M. Yoshida, Y. Yao, G. Zhao, N. Takato, K. Seiguchi, F. Uraguchi, A. Miyashita, N. Ohshima, N. Okada, A. Kawai, J. Wang, G. Yang, and S. Haginoya, Proc. SPIE **6267,** 62671B (2006).
3. J. S. Lawrence, G. R. Allen, M. C. B. Ashley, C. Bonner, S. Bradley, X. Cui, J. R. Everett, L. Feng, X. Gong, S. Hengst, J. Hu, Z. Jian, C. A. Kulesa, Y. Li, D. Luong-Van, A. M. Moore, C. Pennypacker, W. Qin, R. Riddle, Z. Shang, J. W. V. Storey, B. Sun, N. Suntzeff, N. F. H. Tothill, T. Travouillon, C. K. Walker, L. Wang, J. Yan, J. Yang, H. Yang, D. York, X. Yuan, X. G. Zhang, Z. Zhang, X. Zhou, and Z. Zhu, Proc. SPIE **7012,** 701227 (2008).
4. P. Chong, X. Yuan, H. Chen, and D. Wang, A. A. Sin **52,** 5 (2011).
5. K. Lou, Z. Liu, M. W, R. L, P. Q, and R. Zhang, Site Test for Infrared Solar Tower in Yunnan, P. Y. O. 4 (2002).
6. J. W. Hardy, *Adaptive Optics for Astronomical Telescopes* (Oxford University Press, New York, 1998).
7. M. Sarazin and F. Roddier, Astron. Astrophys. **227,** 294 (1990).
8. H. Huang, Y. Yao, and R. Rao, Acta Opt. Sin. (in Chinese) **27,** 8 (2007).
9. D. Rabaud, F. Chazallet, G. Rousset, C. Amra, B. Argast, J. Montri, G. Dumont, B. Sorrente, P. Y. Madec, E. Gendron, R. Arsenault, D. Mouillet, N. Hubin, and J. Charton, Proc. SPIE **4007,** 69 (2008).
10. E. Fedrigo, R. Donaldson, C. Soenke, R. Myers, S. Goodsell, D. Geng, C. Saunter, and N. Dipper, Proc. SPIE **6272,** 627210 (2000).
11. T. Fusco, N. Ageorges, G. Rousset, D. Rabaud, E. Gendron, D. Mouillet, F. Lacombe, G. Zins, J. Charton, C. Lidman, and N. N. Hubin, Proc. SPIE **5490,** 118 (2004).
12. R. J. Noll, J. Opt. Soc. Am. **66,** 207 (1976).
13. D. M. Winker, J. Opt. Soc. Am. A **8,** 1568 (1991).
14. F. Roddier, J. M. Gilli, and G. Lund, J. Opt. **13,** 263 (1982).